Nuclear Magnetic Resonance Study of Pyramidal Inversion and Intramolecular Rearrangements in Complexes of Trimethylplatinum(IV) Halides with Aliphatic and Aromatic Mixed Thio-Seleno-ethers

By **Edward W. Abel, Suresh K. Bhargava, Kenneth Kite, Keith G. Orrell, Vladimir Šik,** and **Bruce L. Williams,** Department of Chemistry, University of Exeter, Exeter EX4 4QD

Mixed chalcogen ligand complexes of trimethylplatinum(IV) halides of general type [$PtXMe_3(MeSRSeMe)$] [R = $(CH_2)_2$ or *o*-C_6H_4] have been prepared and the energy barriers associated with the pyramidal inversions of the individual chalcogen atoms measured by total band-shape dynamic n.m.r. methods. At elevated temperatures an intramolecular scrambling of all of the Pt-methyls occurs, associated with a fluxional movement which apparently effects a 180° rotation of the bidentate ligand.

THIS paper forms part of our studies on the factors governing the energies of pyramidal inversions of Group 6B atoms.[1-8] Dithio- and diseleno-ethers, $MeE(CH_2)_n$-EMe (E = S or Se), have been shown to react with [$(PtXMe_3)_4$] to give either dinuclear complexes when $n = 0$ or 1,[4,6] or mononuclear complexes when $n =$ 2 or 3.[4,5] In the mononuclear complexes the chalcogen atoms have been shown to be inverting essentially independently and all possible invertomer species were detected at low temperatures.[5] In contrast, the inversions of the pairs of chalcogen atoms in the dinuclear species were strongly correlated, if not precisely synchronous, and only the DL invertomer was detected.[6]

Having recently developed synthetic routes to the preparation of mixed S/Se ligands we became interested in assessing how inversion in such mixed S/Se species compared with that in the corresponding dithio- and diseleno-ether complexes. We have reported our findings for the dinuclear $PtXMe_3$ complexes with $MeSCH_2$-SeMe,[8] and now turn our attention to the mononuclear complexes [$PtXMe_3(MeSRSeMe)$] where R = $(CH_2)_2$ or *o*-C_6H_4. In the light of our discoveries of ligand switching and Pt–Me scrambling fluxions in the dinuclear complexes, we have also examined the mononuclear complexes at temperatures well above those for which chalcogen inversions are rapid, in order to find out whether analogous fluxional processes are occurring.

EXPERIMENTAL

Materials.—The trimethylplatinum(IV) halides were prepared as previously described.[8] 1-Methylseleno-2-methylthioethane was prepared by an analogous method to that of methylseleno(methylthio)methane [8] using excess β-chloroethyl methyl sulphide (31.9 g, 0.19 mol). The ligand was a foul smelling pale yellow liquid, b.p. 82 °C (10.0 mmHg *) (yield 12.1 g, 88%). ^1H n.m.r. δ (p.p.m.): 2.05 (Se–Me), 2.16 (S–Me), and 2.8 (CH_2). *o*-Methylselenothioanisole was prepared by a literature method,[9] b.p. 98—99 °C (0.6 mmHg) [lit.,[9] 105—106 °C (1.0 mmHg)]. *o*-Methylthiobenzene thiol [10] (5.0 g, 0.03 mol) was methylated using dimethyl sulphate and sodium hydroxide in methanol to give 1,2-bis(methylthio)benzene. This was extracted with ether, dried and fractionally distilled under reduced pressure, b.p. 76 °C (1 mmHg) [lit.,[10] 78 °C (1 mmHg)] (yield 4.0 g, 74%).

The complexes were prepared by the same general method. The preparation of [$PtClMe_3\{MeS(CH_2)_2SeMe\}$] described below may be taken as typical.

A slight excess of 1-methylseleno-2-methylthioethane (0.1520 g; 0.899 mmol) in chloroform (3 cm^3) was added to trimethylplatinum chloride (0.2380 g; 0.864 mmol †) in chloroform and the resulting solution refluxed for 1 h. The solution was concentrated under vacuum to *ca.* 0.5 cm^3 and light petroleum (b.p. 40—60 °C) added to give a white solid. The solvent was removed and the product recrystallised from chloroform–light petroleum as white crystals of chlorotrimethyl(1-methylseleno-2-methylthioethane)platinum(IV) (yield 0.3152 g, 82%).

Analytical data for the complexes are given in Table 1.

Spectra.—Deuteriochloroform was used as solvent for all the complexes in the temperature range −50 to 90 °C. For higher temperature studies, perdeuterionitrobenzene (C_6D_5-NO_2) was used. A JEOL PS/PFT-100 spectrometer operating at 100 MHz for ^1H studies in the Fourier-transform mode was used. Computations of n.m.r. band-shapes were carried out as previously described.[8]

RESULTS

The S and Se atoms in these five-membered ring complexes are centres of chirality and thus, in the absence of any internal exchange process, four doubly degenerate DL pairs can exist (Figure 1). The difference between this situation and that for the dithio- or diseleno-ether complexes, where two distinct *meso* and one degenerate DL pair of invertomers occur,[5] should be carefully noted. Low-temperature spectra of the mixed S/Se ligand complexes clearly show the existence of these four different DL species. The spectra of [$PtClMe_3\{MeS(CH_2)_2SeMe\}$] are chosen to illustrate the spectra of all the complexes studied.

At *ca.* −50 °C the ligand methyl region, (b) (Figure 2), consisted of eight lines (plus ^{195}Pt satellites), two for each invertomer. Upon warming the sample to *ca.* 80 °C, these lines coalesce in two stages as a result of sulphur inversion and selenium inversion consecutively becoming rapid on the n.m.r. time-scale. In the Pt–Me region, (c)/(d) (Figure 2), twelve signals can be detected at low temperatures (*ca.* −45 °C), four assigned to methyls *trans* to halogen, (d), and eight to methyls *trans* to S and Se, (c). The methyls *trans* to halogen appear at lowest frequency and exhibit larger ^2J(Pt-H) values (73.5—74.5 Hz) compared to those for methyls *trans* to chalcogen (69.0—69.6 Hz). This variation

---

* Throughout this paper: 1 mmHg = (101 325/760) Pa.

† Based on the monomeric unit $PtClMe_3$.

TABLE 1

Characterisation of the complexes

Complex	Colour	M.p./°C	Analysis[a] (%) C	H
$[PtClMe_3\{MeS(CH_2)_2SeMe\}]$	White	175—199[b]	18.85 (18.9)	4.2 (4.25)
$[PtBrMe_3\{MeS(CH_2)_2SeMe\}]$	Yellowish white	220—222	16.95 (17.2)	4.05 (3.9)
$[PtIMe_3\{MeS(CH_2)_2SeMe\}]$	Yellow	183—198[b]	15.65 (15.65)	3.5 (3.55)
$[PtClMe_3\{o\text{-}MeS(C_6H_4)SMe\}]$	White	135	29.6 (29.3)	4.3 (4.35)
$[PtClMe_3\{o\text{-}MeS(C_6H_4)SeMe\}]$	White	126	26.45 (26.7)	3.8 (3.85)
$[PtBrMe_3\{o\text{-}MeS(C_6H_4)SeMe\}]$	White	153	24.25 (24.5)	3.5 (3.55)
$[PtIMe_3\{o\text{-}MeS(C_6H_4)SeMe\}]$	Yellowish white	176	22.4 (22.55)	3.25 (3.25)

[a] Calculated values in parentheses. [b] Decomposes.

in Pt-H coupling has been noted previously[4] and is a useful assignment aid. Detailed chemical shift and spin coupling-constant data are recorded in Table 2. However, individual methyl assignments were not attempted since this region of the spectrum was not used for band-shape studies despite the gross changes (12 lines coalescing to three lines) which occurred on warming to *ca.* 80 °C.

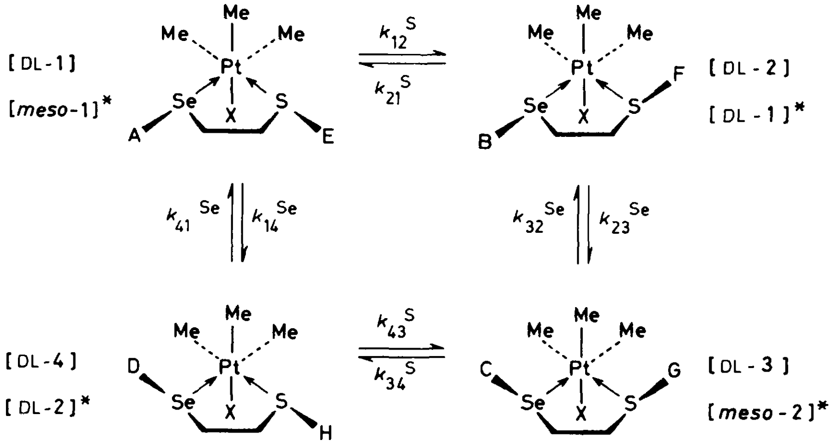

FIGURE 1 Interconversion of isomers by pyramidal inversion of individual S or Se atoms. Only four of the isomers are shown (DL-1—4); their mirror images have identical spectra. An asterisk (*) indicates the nomenclature for the dithio- and diseleno-ether complexes

The methylene region, (a) (Figure 2), was similarly not studied in detail both because of its complexity and also because no information additional to that derived from a detailed analysis of the ligand methyl region would have been obtained. The spectra of the ligand methyl regions for the three different halogen complexes are shown in Figure 3. The assignments shown were based on a careful examination of the chemical shifts and ^3J(Pt-H) values of the dithio- and diseleno-ether analogues.[5] The data pertaining to the latter complexes together with the assignments of the present mixed S/Se complexes are collected in Tables 3 and 4. A high degree of consistency in these data makes the assignments in the present complexes certain. It was observed previously in the homochalcogen complexes[5] that increasing the size of the halogen favoured the less sterically restricted *meso*-2 and DL isomers at the expense of the *meso*-1 isomer, but the usual sequence of populations was *meso*-1 > DL-1 = DL-2 ≫ *meso*-2. By contrast, in the heterochalcogen systems the two DL species with *anti* E-methyls (DL-2 and DL-4) have strikingly different abundances, but their combined abundance outweighs that of DL-1 and DL-3. Increasing the size of the halogen dramatically favours the DL-3 and DL-4 forms at the expense of DL-1 such that the populations change from the order DL-1 > DL-4 > DL-2 > DL-3, for X = Cl, to DL-4 > DL-1 ≈ DL-2 > DL-3, for X = I. This demonstrates the strong preference for the Se–Me group to be in the least sterically hindered conformation.

On raising the temperature of the sample the spectra change as a result of chalcogen inversion in the way depicted in Figure 4. Previous work[5] on the dithio- and diseleno-ether complexes showed that the $\Delta G^{\ddagger}$ values for selenium inversion were of the order of 9—12 kJ mol^{-1} higher than those for sulphur inversion. Furthermore, inversions of like pairs of these chalcogen atoms were shown to be essentially uncorrelated, and therefore in the present complexes it was assumed that S inversion would cause line-shape changes at lower temperatures than would Se inversion. The inversions can be depicted by interconversions between the four DL pairs in a closed circuit, with synchronous double inversion being excluded ($k_{13} = k_{24} = 0$) (Figure 1). In the previous homochalcogen complexes[5] it was necessarily true that the rate constant $k_{12} = k_{14}$ and k_{32}* $= k_{34}$, but it was further assumed that all four rate constants were the same. An analogous assumption was initially made here, namely that $k_{12}^S = k_{34}^S$ and $k_{14}^{Se} = k_{32}^{Se}$ but this was found to lead to unsatisfactory band-shape fits and the fittings were therefore based on two different S inversion rates and two Se inversion rates (but see later). The chalcogen methyls were labelled A—H as

* In ref. 5, this rate constant was erroneously quoted as k_{23}.

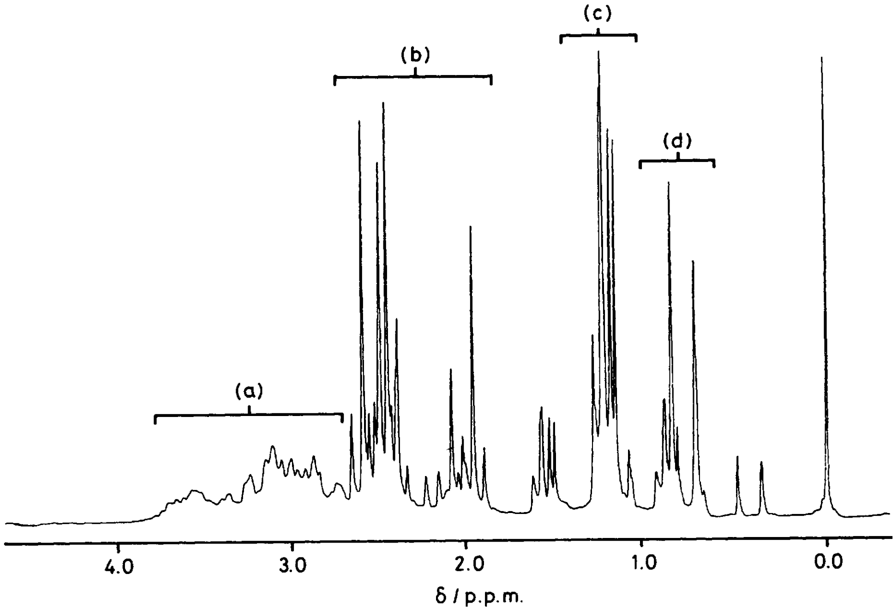

FIGURE 2 Total 100 MHz ^{1}H spectrum of [PtClMe$_3${MeS(CH$_2$)$_2$SeMe}] at −46 °C

TABLE 2

Chemical shifts [a] and spin coupling constants of PtMe protons in the slow and fast inversion limits

		PtMe (*trans* to S,Se)		PtMe (*trans* to X)	
Complex [b]	*T*/°C	δ/p.p.m.	^2J/Hz	δ/p.p.m.	^2J/Hz
[PtClMe$_3${MeS(CH$_2$)$_2$SeMe}]	−46.2	1.19, 1.21, 1.24, 1.25, 1.26, 1.28, 1.30, 1.31	69.1, 69.6, 69.6, 69.0, 69.0, 69.6, 69.0, 69.0	0.70, 0.73, 0.74, 0.87	73.8, 74.7, 74.5, 73.6
	88.4	1.27, 1.28	70.0, 70.1	0.76	73.1
[PtBrMe$_3${MeS(CH$_2$)$_2$SeMe}]	−38.4	1.28, 1.30, 1.33, 1.34, 1.36, 1.39	69.3, 69.9, 69.3, 69.6, 69.4, 69.3	0.80, 0.82, 0.84, 0.95	73.9, 72.9, 73.6 72.6
	86.8	1.48	70.6	0.88	72.0
[PtIMe$_3${MeS(CH$_2$)$_2$SeMe}]	−58.0	1.45, 1.48, 1.50, 1.55	69.7, 69.9, 69.9, 69.9	0.94, 0.96, 0.98, 1.06	70.0, 71.4, 71.3, 70.2
	80.3	1.52, 1.53	71.0, 71.3	0.98	69.9
[PtClMe$_3${*o*-MeS(C$_6$H$_4$)SMe}]	−77.8	1.22, 1.25, 1.30	69.3, 69.6, 69.0	0.75, 0.86, 0.88	73.9, 73.2, 72.8
[c]	49	1.48	70.3	0.86	71.8
[PtClMe$_3${*o*-MeS(C$_6$H$_4$)SeMe}]	−78	1.32, 1.34, 1.35, 1.40	69.8, 69.3, 70.1, 69.1	0.80, 0.90, 0.92, 0.97	73.7, 73.7, 73.5, 73.0
[c]	56	1.50, 1.51	70.1, 70.9	0.87	71.9
[PtBrMe$_3${*o*-MeS(C$_6$H$_4$)SeMe}]	−83.4	1.33, 1.37, 1.39	69.8, 70.6, 69.6	0.88, 0.98, 1.00, 1.04	73.0, —, 72.7, 71.5
[c]	47.4	1.58, 1.60	70.4, 71.4	0.99	71.4
[PtIMe$_3${*o*-MeS(C$_6$H$_4$)SeMe}]	−71.5	1.45, 1.47, 1.50, 1.54	70.3, 71.0, 71.1, 70.6	1.05, 1.10, 1.12, 1.17	71.3, —, —, 71.5
[c]	56.5	1.71, 1.74	70.9, 71.7	1.20	69.7

[a] Chemical shifts relative to SiMe$_4$. [b] Solvent for aliphatic complexes was CDCl$_3$ and for aromatic complexes, CD$_2$Cl$_2$. [c] Solvent was C$_6$D$_5$NO$_2$.

in Figure 1; and since there were no detectable SMe–SeMe proton spin interactions the dynamic spin problem was represented as the sum of five sub-spin problems (see below).

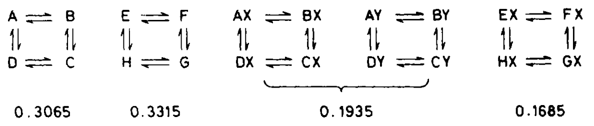

In this scheme, X = ^{195}Pt and Y = ^{77}Se. The numbers below the sub-spin systems represent the normalised weighting factors used in the computations. Since no ^{77}Se satellites were separately detected, implying that ^2J(Se–H) ≈ ^3J(Pt–H), the Se-methyl satellite spectrum was treated as a ^{195}Pt satellite spectrum with an enhanced intensity due to the natural abundance (7.6%) of ^{77}Se. After determining the static parameters of the chalcogen methyls and any temperature dependences of these parameters, computer simulated spectra were obtained and compared with the experimental spectra (Figure 4). It will be observed that on raising the temperature to *ca.* 5 °C certain bands broadened and coalesced as a result of S inversion. However, two distinct Se-methyl signals were observed throughout this temperature range implying that Se inversion was still slow. This inversion rate, however, increased with temperature such that at *ca.* 94 °C (Figure 5) a second coalescence phenomenon occurred, and by *ca.* 160 °C had become very fast on the n.m.r. time-scale. Pt–E–Me coupling was retained even

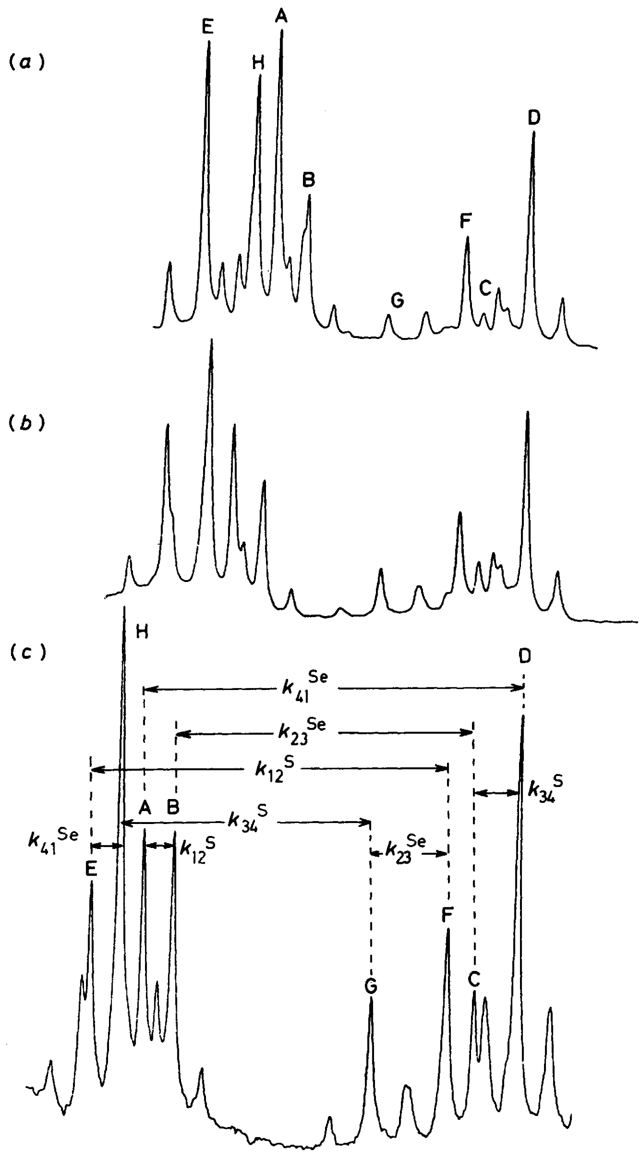

FIGURE 3 Ligand methyl ^{1}H spectra of [PtXMe$_3${MeS(CH$_2$)$_2$SeMe}], X = Cl (*a*), Br (*b*), and I (*c*), at low temperature showing halogen dependence of invertomer populations and line assignments to individual invertomers. Lines are labelled according to Figure 1: A,E [DL-1]; B,F [DL-2]; C,G [DL-3]; and D,H [DL-4]

at this highest temperature confirming a non-dissociative inversion mechanism. Excellent fits of these complex band-shapes were achieved using 4 independent rate constants (*N.B.*, in practice, only 2 non-zero *k* values were required for some temperatures) and the 'best-fit' values are listed in Table 5.

At temperatures above *ca.* 100 °C gross broadenings and eventual coalescence of *all* the Pt-Me signals occurred (Figure 5). This change, which was perfectly reversible and retained the Pt-Me couplings, can only arise from some type of intramolecular scrambling of the methyl environments analogous to that observed in the dinuclear Pt^{IV} complexes.[6] In the latter we have shown that this methyl scrambling accompanies a ligand switching fluxion between the Pt atom pairs. In the present mononuclear complexes at temperatures above *ca.* 100 °C, the ligand methylene region changes from its original complex ABCD-type structure [region (a), Figure 2] to one characteristic of an AA′BB′ system, Pt coupling being retained throughout. Such a change implies a fluxion which appears to effect a 180° switching of the ligand about a single platinum atom. Simultaneously, there is a scrambling of all three platinum methyls. The transition state for the ligand switching (or 'pancaking') process is likely to be a highly fluxional pseudo-eight-co-ordinate species in which such methyl scrambling would occur. If the two motions are not strongly correlated it should, in theory, be possible to detect them separately since the 'pancaking' process will average only the Pt-methyls *trans* to ligand (labelled R,S below) whereas the scrambling process will also interconvert the methyl *trans* to halogen (labelled T below). The spin problem is therefore that shown below (X = ^{195}Pt) where k_1 and k_2 are

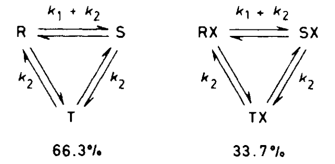

the rate constants for the 'pancaking' and scrambling processes respectively. If the processes are correlated, as we have suggested is the case with the dinuclear complexes, then the three Pt-methyls will interconvert at the same rate k_1 ($= k_2$). Unfortunately, in the present complexes it was not possible to decide between these two situations since the chemical shifts of R and S were too similar for the spectra to be sensitive to the rate of R $\rightleftharpoons$ S exchange (be it at a rate $k_1 + k_2$, or k_1). No direct evidence for this 'pancaking' movement was therefore obtained. Nevertheless, such a movement is still thought to be the basic prerequisite for methyl scrambling. We are currently examining other complexes where this fluxional process might be more in evidence. The static parameters used for the band-shape fittings (Figure 5) are given in Table 6.

DISCUSSION

Pyramidal Inversion.—The Arrhenius and thermodynamic activation parameters for pyramidal inversion in these mixed S/Se ligand complexes are presented in Table 7. Comparison of the $\Delta G^{\ddagger}$ values (which are least prone to systematic error) with those for sulphoxides [11] and selenoxides [12] reveals a striking reduction in magnitude when the chalcogens are co-ordinated to Pt^{IV}, which we attribute to appreciable stabilisation of the transition-state structure by $(p-d)\pi$ overlap. The inversion energies in the above aliphatic ligand complexes are of very similar magnitude to those for the dithio- and diseleno-ether complexes (*cf.* Table 3, ref. 5) as was expected. However, replacement of the aliphatic backbone of the ligand by the aromatic moiety o-C$_6$H$_4$ lowers the $\Delta G^{\ddagger}$ values for S and Se inversion by *ca.* 10—11 kJ mol^{-1} and *ca.* 7—8 kJ mol^{-1} respectively. This is also certainly the result of $(p-p)\pi$ conjugation between the chalcogen lone pair and the ligand backbone, which is more effective in the planar transition state than in the pyramidal ground state. Our results suggest that

TABLE 3

Static parameters used [a] in the calculation of pyramidal inversion energies in the complexes $[PtXMe_3\{MeE(CH_2)_2E'Me\}]$

			[*meso*-1] [b]/[DL-1] [c]			[DL-1] [b]/[DL-2] [c]			[DL-2] [b]/[DL-4] [c]			[*meso*-2] [b]/[DL-3] [c]			
X	E	E′	ν	^{3}J	p	ν	^{3}J	p	ν	^{3}J	p	ν	^{3}J	p	T_2^*/s
Cl	S	S	259.1	12.7	0.595	209.9	15.3	0.190	252.2	12.5	0.190	212.8	15.3	0.025	0.265
Cl	Se	Se	247.2	9.9	0.388	240.2	9.9	0.274	192.3	11.9	0.274	203.3	11.9	0.065	0.367
Cl	S	Se	259.7 246.2	13.0 9.6	0.460	210.5 240.4	15.3 10.4	0.166	250.0 198.5	12.4 12.1	0.337	225.2 207.2	15.0 12.5	0.037	0.250
Br	S	S	267.0	13.2	0.358	208.6	15.5	0.295	261.0	13.2	0.295	215.1	15.5	0.054	0.106
Br	Se	Se	254.5	10.4	0.257	247.6	10.4	0.315	192.8	11.8	0.315	203.4	11.8	0.117	0.367
Br	S	Se	266.7 254.2	13.4 10.4	0.310	211.8 248.4	15.3 10.4	0.186	258.8 199.3	13.3 12.2	0.407	226.4 207.2	14.8 12.1	0.097	0.250
I	S	S	277.7	13.9	0.295	210.4	15.6	0.303	272.9	14.1	0.303	220.1	15.3	0.100	0.245
I	Se	Se	267.6	12.0	n.c.	260.7	11.3	n.c.	193.6	12.2	n.c.	204.9	12.1	n.c.	n.c.
I	S	Se	277.3 268.2	14.3 12.0	0.217	209.6 262.6	15.6 11.3	0.193	272.1 196.2	14.2 12.3	0.450	222.9 204.1	15.3 12.0	0.140	0.240

[a] Chemical shifts (ν/Hz) of E methyls measured relative to $SiMe_4$; ^{3}J represents $^{3}J(^{195}Pt–E–C–^{1}H)$/Hz; p = isomer populations (±0.005); T_2^* = effective spin–spin relaxation time; n.c. = not calculated. [b] Nomenclature for dithio- and diseleno-ether complexes [see Figure 1(*)] [c] Nomenclature for mixed chalcogen ligand complexes (see Figure 1).

TABLE 4

Static parameters [a] for the complexes $[PtXMe_3\{o\text{-}MeE(C_6H_4)E'Me\}]$

			[*meso*-1] [b]/[DL-1] [c]			[DL-1] [b]/[DL-2] [c]			[DL-2] [b]/[DL-4] [c]			[*meso*-2] [b]/[DL-3] [c]			
X	E	E′	ν	^{3}J	p	ν	^{3}J	p	ν	^{3}J	p	ν	^{3}J	p	T_2^*/s
Cl	S	S	297.5	13.5	0.452	293.0	13.0	0.231	293.0	13.0	0.231	259.6	16.0	0.086	0.180
Cl	S	Se	296.5 282.5	13.2 10.7	0.370	250.0 277.7	15.2 10.2	0.165	291.9 229.4	13.1 12.1	0.355	260.3 239.3	16.1 12.7	0.110	0.191
Br	S	Se	305.5 292.2	14.5 12.0	0.225	248.7 287.4	15.4 11.3	0.188	301.6 227.1	14.0 12.5	0.397	259.4 237.7	15.6 12.7	0.190	0.160
I	S	Se	317.4 305.1	14.6 12.3	0.125	247.6 300.2	15.1 12.0	0.180	312.7 224.6	14.9 12.0	0.415	257.8 235.5	16.4 12.3	0.280	0.140

[a] Chemical shifts (ν/Hz) of E-methyls measured relative to $SiMe_4$; ^{3}J represents $^{3}J(^{195}Pt–E–C–H)$/Hz; p = isomer populations (±0.005). [b] Nomenclature for dithio-ligand complex. [c] Nomenclature for mixed chalcogen ligand complexes.

TABLE 5

'Best fit' rate constants used for the simulation of the spectra shown in Figure 4

Spectrum no.	Temp./°C	Rate constants, k/s^{-1} k_{12}^{S}	k_{34}^{S}	k_{23}^{Se}/k_{14}^{Se}
(*a*)	−47.0	0.001	0.001	0.000
(*b*)	−14.2	2.1	33.9	0.000
(*c*)	−9.3	4.0	60.3	0.000
(*d*)	0.4	11.7	170.0	0.000
(*e*)	4.8	18.6	300	0.000
(*f*)	21.3	93.3	1 202	0.000
*	38.0	450	5 000	3.5
*	47.5	900	10 000	6.6
(*g*)	57.0	1 905	15 000	14.2
(*h*)	65.2	3 250	15 000	28.9
*	72.8	5 000	15 000	56.0

* Spectra not shown in Figure 4.

the $(3p–2p)\pi$ delocalisation in the case of S inversion is slightly more extensive than the $(4p–2p)\pi$ delocalisation associated with Se inversion. These trends closely parallel those found by Mislow and co-workers [13,14] for phosphorus and arsenic inversion. More extensive studies of the effects of π delocalisation on S inversion in a variety of transition-metal complexes will be published elsewhere.[15]

A notable difference between the homo- and hetero-chalcogen ligand complexes is that in the former case [5] only single magnitudes of S or Se inversion were quoted whereas in the latter complexes two different S inversion barriers have been computed each time. The differences in these S inversion energies vary from *ca.* 6 kJ mol^{-1} for the chloro-complex to *ca.* 1 kJ mol^{-1} for the iodo-complex. Such differences are attributed primarily (but not solely) to the different ground-state energies of the invertomers. These energies have been calculated using the standard thermodynamic equation $\Delta G^{\ominus} = -RT\ln K^{\ominus}$ where $K^{\ominus}$ is the ratio of the population of the chosen DL invertomer to that of DL-1. These values are displayed in Figure 6. The trends can be interpreted in terms of the relative sizes of halogen and methyl groups.

TABLE 6

Static parameters used in calculating the PtMe scrambling energy barriers

		PtMe (*trans* to S)		PtMe (*trans* to Se)		PtMe (*trans* to X)		
Complex [a]	T/°C	ν/Hz	^{2}J/Hz	ν/Hz	^{2}J/Hz	ν/Hz	^{2}J/Hz	T_2^*/s
$[PtClMe_3\{MeS(CH_2)_2SeMe\}]$	94.1	139.8	70.7	139.8	70.7	79.2	72.4	0.170
$[PtBrMe_3\{MeS(CH_2)_2SeMe\}]$ [b]	83.9	150.9	70.8	150.9	70.8	85.0	72.0	0.367
$[PtIMe_3\{MeS(CH_2)_2SeMe\}]$ [b]	87.9	169.5	71.0	169.5	71.0	100.2	69.6	0.344
$[PtClMe_3\{o\text{-}MeS(C_6H_4)SMe\}]$	49.0	147.5	70.3			86.2	71.8	0.520
$[PtClMe_3\{o\text{-}MeS(C_6H_4)SeMe\}]$	68.0	150.7	70.9	149.1	70.3	86.6	70.0	0.260
$[PtBrMe_3\{o\text{-}MeS(C_6H_4)SeMe\}]$	81.2	158.9	71.4	157.2	70.4	97.5	71.4	0.400
$[PtIMe_3\{o\text{-}MeS(C_6H_4)SeMe\}]$	78.1	173.2	72.0	170.9	70.9	113.5	69.7	0.280

[a] Solvent was $C_6D_5NO_2$; chemical shifts measured relative to $SiMe_4$. [b] Solvent was $C_6D_5NO_2–C_6D_6$.

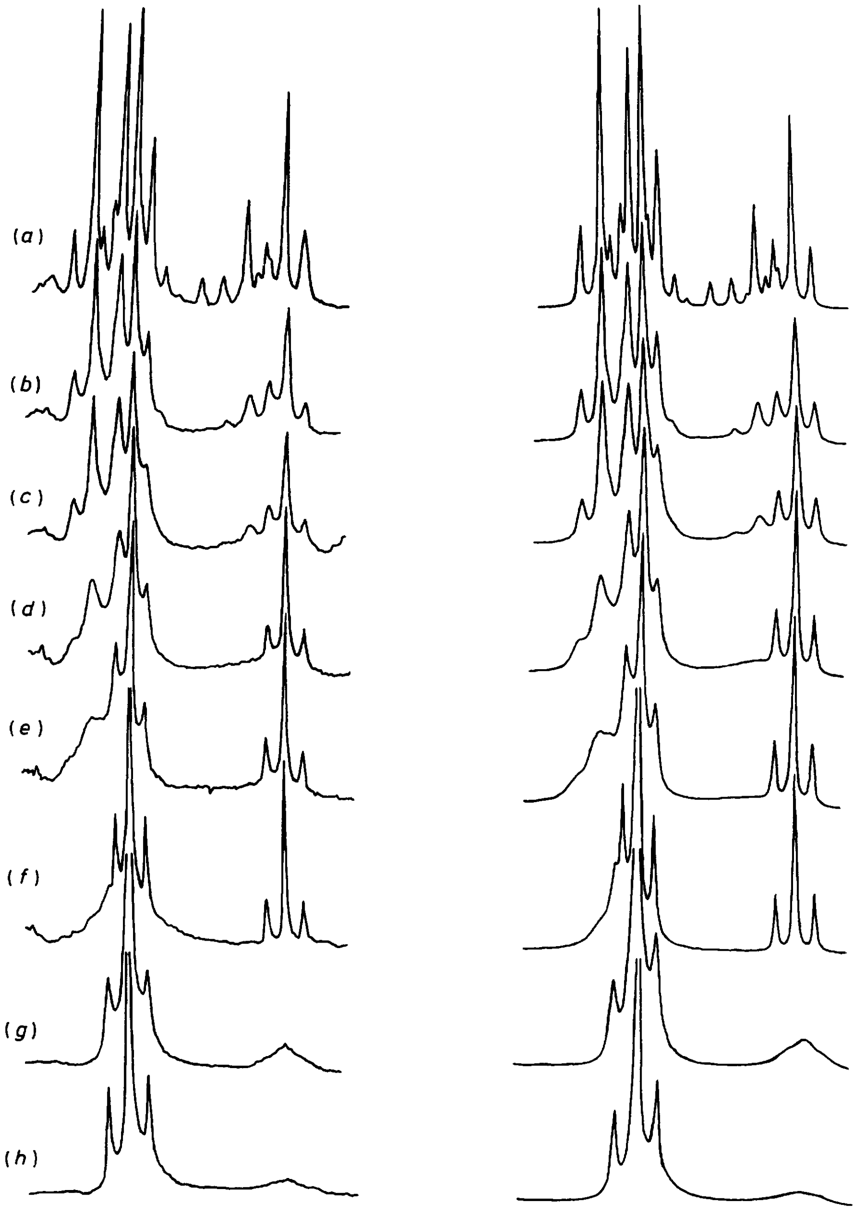

FIGURE 4 Experimental and computer simulated ^1H spectra (see Table 5) of $[PtClMe_3\{MeS(CH_2)_2SeMe\}]$ showing the effects of chalcogen (predominantly sulphur) inversion

In the chloro-complex, where there is an appreciable disparity in size, there is substantial relative stabilisation of certain ground-state configurations (up to *ca.* 5 kJ mol^{-1}) and the S inversion energies differ by *ca.* 6 kJ mol^{-1}. However, in the iodo-complex, where the two groups are more comparable in size, the invertomer populations are more equal and the S inversion energies are of a similar magnitude.

The origin of the multiplicity of barrier energies may be seen by sketching the likely forms of potential-energy profiles for both the homo- and hetero-chalcogen complexes. For the dithio- and diseleno-ether complexes there will be *three* different-energy ground states and and *two* different transition states (see below).

In this system there is clearly no reason why the (*meso*-1 ⟶ DL-1) barrier should be identical to that of (DL-1 ⟶ *meso*-2). The computation should therefore be performed using different rate constants k and k' for these two interconversions, as shown in the Scheme below (p_2 = population of DL-1, p_3 = population of *meso*-2). In practice, however, it was found that the spectral line-shapes were sensitive to only a single magnitude of rate constant, except in one or two cases at lower temperatures. Only single magnitudes of chalcogen inversion barriers were therefore computed, any energy difference between the two theoretical types being estimated to be no greater than 1—2 kJ mol^{-1}.

The potential energy profile for the heterochalcogen

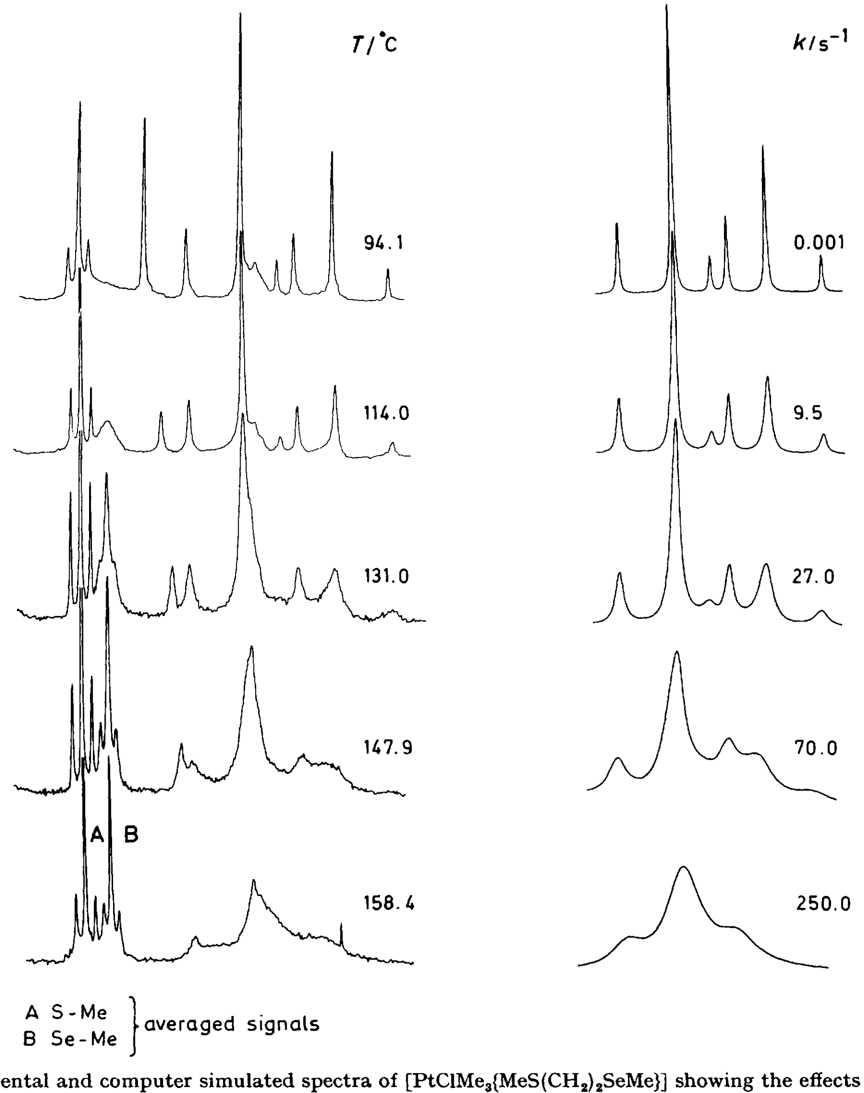

FIGURE 5 Experimental and computer simulated spectra of [$PtClMe_3\{MeS(CH_2)_2SeMe\}$] showing the effects of selenium inversion and Pt-methyl scrambling; *k* values refer to the scrambling process

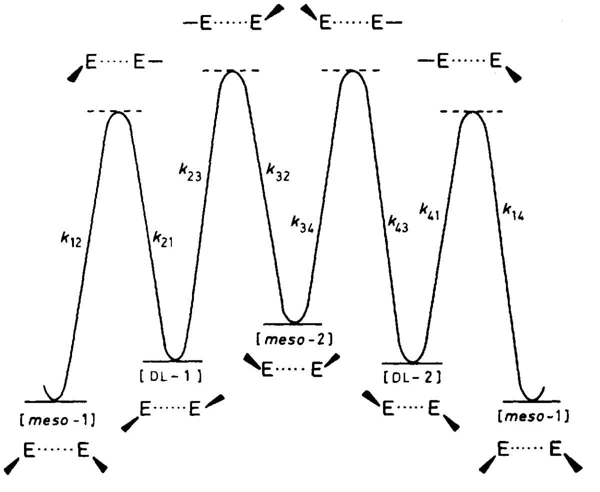

ligand complexes can be represented as shown below. Since all four invertomers are chemically distinct there are now *four* different ground states and *four* different transition states. This implies four different energy barriers, two associated with S inversion and two for Se inversion. Two different S inversion barriers were computed from the spectral changes of the E-methyl region in the temperature range —47 to 57 °C [Figure 4, spectra (*a*)—(*f*)]. However, before S inversion becomes very fast on the n.m.r. time-scale, Se inversion starts affecting the observed line-shapes and thus the simulations of the spectra in the higher temperature range 35 to 75 °C have to be based on four non-zero rate constants,

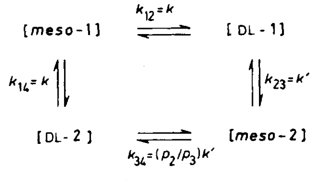

SCHEME

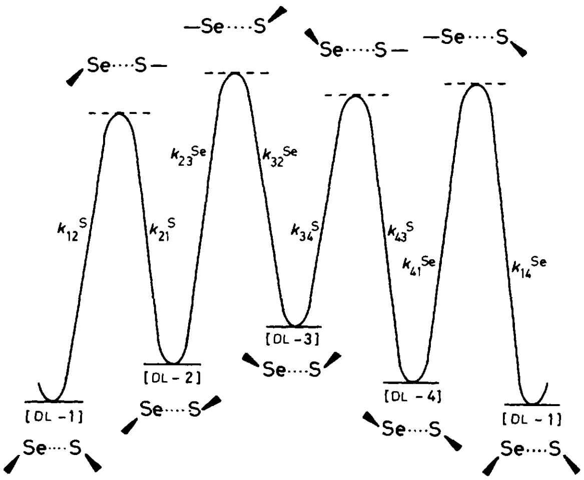

two for S inversion and two for Se inversion. The choice of the pairs of ' best fit ' Se inversion rate constants (k_{14} and k_{23}) posed considerable difficulties. This arose from the fact that in the present spectra the S and Se inversions were almost (but not quite) independently measurable. If they had been so, it would have been possible to reformulate the spin problem after S inversion has become rapid in terms of an interconversion between two spin configurations (one being the average of the invertomer pairs DL-1 and DL-2 and the other the average of DL-3 and DL-4). In such circumstances the spectra would be sensitive to only a single set of Se rate constants from which a single magnitude of Se barrier could be computed. This approach effectively denies any distinction between the two theoretically possible Se barrier energies. In actual fact, such a treatment was not possible and two values of Se rate constants were required for each computation of the four-configuration spin problem. However, it was subsequently found that the spectral line-shapes depended to a good approximation only on the *sum* of the rate constants k_{14} and k_{23} and not on their individual values. These rate constants were therefore for convenience given equal values at any particular temperature. Such a treatment can be shown to be equivalent to the previous case where the two types of chalcogen inversion were assumed to be separable, and resulted in a single magnitude of Se energy barrier being deduced.

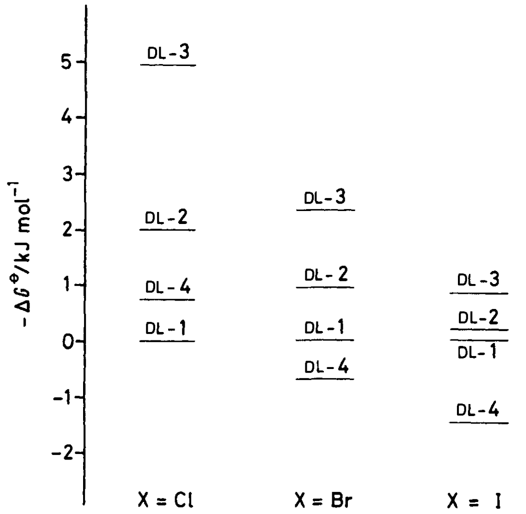

FIGURE 6 Relative ground state energies (ΔG°) of the various invertomers of [PtXMe$_3${MeS(CH$_2$)$_2$SeMe}]. Values calculated at 233 K relative to DL-1 invertomer

Fluxional Rearrangements.—The energies associated with the scrambling of the Pt-methyl environments are shown in Table 8. These values are of the order of 20 kJ mol^{-1} higher than those of Se inversion and are essentially halogen independent. It should again be noted that the values for the aromatic ligand complexes are lower (by *ca.* 6—7 kJ mol^{-1}) than for the aliphatic complexes.

A variety of mechanisms can be proposed to explain this methyl scrambling. One mechanism involves halogen dissociation–recombination *via* a highly non-rigid five-co-ordinate intermediate which would allow the Pt-methyls to scramble. Such a mechanism would be completely reversible with temperature and would not involve any Pt–Me bond breaking so that ^{195}Pt–H couplings would be retained. As it was not possible to directly study the halogen resonances, the following halogen exchange experiment was performed. To a solution of [PtClMe$_3${MeS(CH$_2$)$_2$SeMe}] in $C_6D_5NO_2$ at 150 °C (at which temperature methyl scrambling is fast on the n.m.r. time-scale) a mol equivalent of KI was added. Hydrogen-1 n.m.r. spectra taken both before and after addition, and then at room temperature, showed little evidence of halogen exchange. Furthermore, a halogen dissociation–recombination mechanism would very likely be reflected in a halogen dependence of the scrambling energy barriers but no such trend was found (Table 8); nor does such mechanism explain the strikingly different scrambling energies of the aliphatic and aromatic ligand complexes.

An alternative mechanism involving a five-co-ordinate intermediate can be envisaged involving the breaking and reforming of *individual* Pt–E bonds. In this mechanism the Pt–E–Me spin couplings would either be approximately halved in magnitude (homochalcogen complexes) or become zero (heterochalcogen complexes). Since no reduction in ^3J(Pt–Me) values was observed in the appropriate temperature range this mechanism can also be discounted.

The mechanism we favour involves the formation of a highly fluxional pseudo-eight-co-ordinate Pt^{IV} intermediate[16] by ligand rotation through 180° (Figure 7). Such a ' pancaking ' movement is analogous to the ligand switching movement proposed for the dinuclear Pt^{IV} complexes.[6,8] However, as we have mentioned earlier, it has not proved possible to date to obtain direct evidence for this ' pancaking ' movement but we are currently pursuing this problem further. In this context it is of interest to note that *two* barrier energies for this ligand movement are theoretically possible depending on the nature of the pseudo-eight-co-ordinate inter-

TABLE 7

Arrhenius and thermodynamic activation parameters for sulphur and selenium inversion in the mixed chalcogen ligand complexes

Complex	Inversion	E_a/kJ mol^{-1}	$\log_{10}A$	$\Delta G^{\ddagger}$ [e]/ kJ mol^{-1}	$\Delta H^{\ddagger}$/ kJ mol^{-1}	$\Delta S^{\ddagger}$/ J K^{-1} mol^{-1}
$[PtClMe_3\{MeS(CH_2)_2SeMe\}]$	S^1 [a]	68.0 ± 0.3	14.1 ± 0.1	60.8 ± 0.1	65.8 ± 0.3	16.9 ± 1.2
	S^2 [b]	62.3 ± 1.2	14.1 ± 0.2	54.9 ± 0.2	60.1 ± 1.2	17.6 ± 4.5
	Se [c]	71.3 ± 3.1	12.5 ± 0.5	73.1 ± 0.3	68.6 ± 3.1	−15.2 ± 9.3
$[PtIMe_3\{MeS(CH_2)_2SeMe\}]$	S^1	69.0 ± 0.7	14.4 ± 0.1	60.0 ± 0.1	66.8 ± 0.7	22.7 ± 2.6
	S^2	61.1 ± 1.9	13.2 ± 0.4	58.9 ± 0.2	58.8 ± 1.7	−0.1 ± 6.9
	Se	77.5 [d]	13.5	73.5 [d]	74.7 [d]	3.7
$[PtBrMe_3\{o\text{-}MeS(C_6H_4)SeMe\}]$	S^1	52.2 ± 0.6	13.3 ± 0.1	49.6 ± 0.1	50.2 ± 0.6	2.2 ± 2.5
	S^2	50.4 ± 0.2	13.2 ± 0.1	47.8 ± 0.1	48.3 ± 0.2	1.8 ± 0.8
	Se	67.1 ± 0.7	13.6 ± 0.1	65.7 ± 0.1	64.5 ± 0.7	−4.1 ± 2.4
$[PtClMe_3\{o\text{-}MeS(C_6H_4)SMe\}]$	S	51.8 ± 0.4	12.7 ± 0.1	52.2 ± 0.1	49.9 ± 0.4	−7.7 ± 1.8

[a] [DL-1] $\longrightarrow$ [DL-2]. [b] [DL-3] $\longrightarrow$ [DL-4]. [c] Assuming the Se barriers [DL-2] $\longrightarrow$ [DL-3] and [DL-1] $\longrightarrow$ [DL-4] are equal. [d] Only approximate (±1 kJ mol^{-1}) values available due to overlapping of $-CH_2-$ and PtEMe regions and to non-linear isomer population and chemical shift changes with temperature. [e] At 298.15 K.

TABLE 8

Energy barriers calculated for the PtMe scrambling process

Complex	E_a/kJ mol^{-1}	$\log_{10}A$	$\Delta G^{\ddagger}$ */ kJ mol^{-1}	$\Delta H^{\ddagger}$/ kJ mol^{-1}	$\Delta S^{\ddagger}$/ J K^{-1} mol^{-1}
$[PtClMe_3\{MeS(CH_2)_2SeMe\}]$	94.0 ± 3.8	13.6 ± 0.5	89.2 ± 0.9	90.7 ± 3.8	5.0 ± 9.6
$[PtBrMe_3\{MeS(CH_2)_2SeMe\}]$	94.0 ± 3.6	13.7 ± 0.5	88.8 ± 1.0	90.6 ± 3.6	6.0 ± 8.8
$[PtIMe_3\{MeS(CH_2)_2SeMe\}]$	99.5 ± 1.5	14.5 ± 0.2	89.6 ± 0.4	96.3 ± 1.5	22.4 ± 3.8
$[PtClMe_3\{o\text{-}MeS(C_6H_4)SMe\}]$	83.6 ± 1.0	12.7 ± 0.1	83.8 ± 1.8	80.4 ± 1.0	−11.4 ± 2.6
$[PtClMe_3\{o\text{-}MeS(C_6H_4)SeMe\}]$	85.1 ± 1.0	13.0 ± 0.1	83.8 ± 0.2	81.9 ± 1.0	−6.3 ± 2.6
$[PtBrMe_3\{o\text{-}MeS(C_6H_4)SeMe\}]$	84.5 ± 0.8	12.9 ± 0.1	83.7 ± 0.2	81.3 ± 0.8	−8.2 ± 2.1
$[PtIMe_3\{o\text{-}MeS(C_6H_4)SeMe\}]$	86.1 ± 1.0	13.1 ± 0.1	84.2 ± 0.2	82.9 ± 1.0	−4.6 ± 2.5

* At 298.15 K.

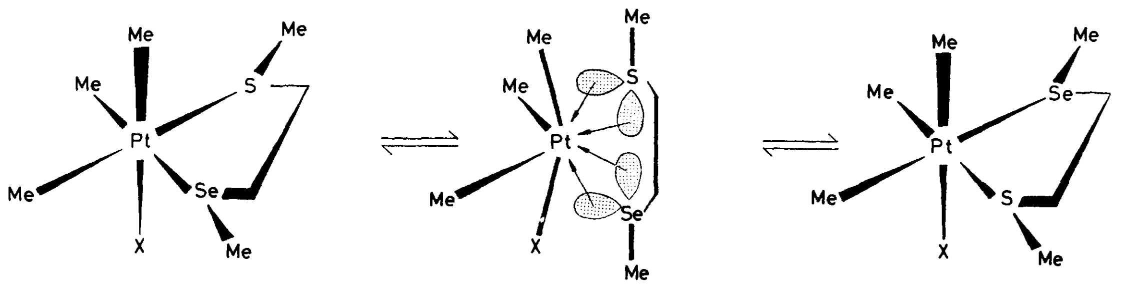

FIGURE 7 Proposed mechanism for the 180° 'pancake' rotation of the ligand

mediate consequent on the direction of rotation of the ligand. Indirect evidence in support of the pseudo-eight-co-ordinate intermediate comes from the observation that the Pt^{IV} diphosphine complex $[PtClMe_3(Ph_2PCH_2CH_2PPh_2)]$ does *not* undergo any Pt-methyl scrambling up to *ca.* 125 °C when ligand dissociation occurs. This can be rationalised in terms of the shortage of lone pairs on phosphorus to form a pseudo-eight-co-ordinate Pt^{IV} species necessary to activate the methyl scrambling. A five-co-ordinate Pt^{IV} diphosphine intermediate is, however, electronically quite feasible although its energy could be somewhat higher than the five-co-ordinate chalcogen intermediates. We are therefore inclined to the view that the stereochemical rigidity of the diphosphine complex provides indirect support for a pseudo-eight-co-ordinate Pt^{IV} intermediate in the present complexes.

When describing the interconversions between the various static structures of these complexes as a result of chalcogen inversions, we limited the discussion to individual diastereoisomers of the four DL pairs (Figure 1) since their mirror image counterparts are n.m.r.-indistinguishable. When, however, our description of the dynamic stereochemistry encompasses the chalcogen inversions and the ligand 'pancake' rotations, all eight diastereoisomers need to be considered. These are most conveniently represented by a Desargues–Levi graph, which in this case is in the form of a simple cube (Figure 8). On the front face of the cube four isomers are shown as in Figure 1. Their non-superimposable mirror images are in the diametrically opposite corners of the back face of the cube. The pyramidal inversion energies are different depending on which front edge of the cube is traversed; the four energies associated with the back face are, of course, the same as those for the front face. In order to move between the front and back faces the molecule has to undergo a 'pancake flip'. Closer examination of the diagram reveals that for any species

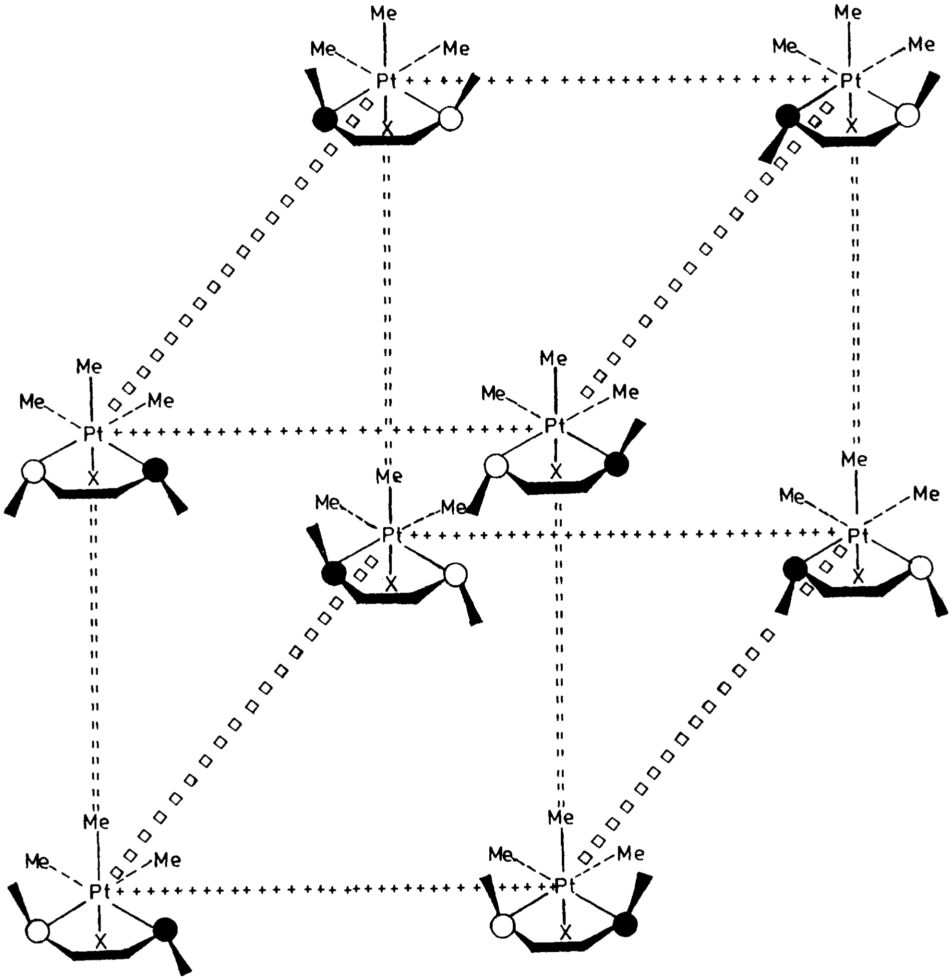

FIGURE 8 Desargues–Levi graph for the interconversion of the eight diastereoisomers of [PtXMe$_3${MeS(CH$_2$)$_2$SeMe}]: S inversion (+++), Se inversion (===), pancake flip (□□□)

to change to its mirror image configuration it has to undergo inversion at sulphur, inversion at selenium, and a ' pancake flip ', although not necessarily in that order. In this way the diagram provides a unified picture of the main fluxional properties of these Pt^{IV} complexes.

We are indebted for the generous support of the Commonwealth Scholarship Commission U.K., and the University Grants Commission, India (to S. K. B.).

[1/1215 *Received, 3rd August*, 1981]

REFERENCES

[1] E. W. Abel, G. W. Farrow, and K. G. Orrell, *J. Chem. Soc., Dalton Trans.*, 1976, 1160.

[2] E. W. Abel, G. W. Farrow, K. G. Orrell, and V. Šik, *J. Chem. Soc., Dalton Trans.*, 1977, 42.

[3] E. W. Abel, A. K. Ahmed, G. W. Farrow, K. G. Orrell, and V. Šik, *J. Chem. Soc., Dalton Trans.*, **1977**, 47.

[4] E. W. Abel, A. R. Khan, K. Kite, K. G. Orrell, and V. Šik, *J. Chem. Soc., Dalton Trans.*, 1980, 1169.

[5] E. W. Abel, A. R. Khan, K. Kite, K. G. Orrell, and V. Šik, *J. Chem. Soc., Dalton Trans.*, 1980, 1175.

[6] E. W. Abel, A. R. Khan, K. Kite, K. G. Orrell, and V. Šik, *J. Chem. Soc., Dalton Trans.*, 1980, 2208, 2220.

[7] E. W. Abel, M. Booth, G. King, G. M. Pring, K. G. Orrell, and V. Šik, *J. Chem. Soc., Dalton Trans.*, 1981, 1846.

[8] E. W. Abel, K. Kite, K. G. Orrell, V. Šik, and B. L. Williams, *J. Chem. Soc., Dalton Trans.*, 1981, 2439.

[9] C. G. Pierpont, B. J. Corden, and R. Eisenberg, *Chem. Commun.*, 1969, 401.

[10] S. E. Livingstone, *J. Chem. Soc.*, 1956, 437.

[11] D. R. Rayner, A. J. Gordon, and K. Mislow, *J. Am. Chem. Soc.*, 1968, **90**, 4854.

[12] M. Oki and H. Iwamura, *Tetrahedron Lett.*, 1966, 2917.

[13] W. Egan, R. Tang, G. Zon, and K. Mislow, *J. Am. Chem. Soc.*, 1971, **93**, 6205.

[14] R. H. Bowman and K. Mislow, *J. Am. Chem. Soc.*, 1972, **94**, 2861.

[15] E. W. Abel, S. K. Bhargava, K. Kite, K. G. Orrell, V. Šik, and B. L. Williams, unpublished work.

[16] E. L. Muetterties, *Acc. Chem. Res.*, 1970, **3**, 266.